Analysis of a Wind Turbine Blade Profile for Tapping Wind Power at the Regions of Low Wind Speed

Dr. S. P. Vendan[1], S. Aravind Lovelin[2], M. Manibharathi[2] and C. Rajkumar[2]

[1] Associate Professor,

[2] IV Year BE Mechanical Engineering, Department of Mechanical Engineering,

PSG College of Technology, Coimbatore,

Tamilnadu, India

Abstract. The project is aimed at designing a wind turbine for tapping the low speed wind in urban locations. It is to be noted that most of the high wind power density regions in the zone of high wind speed are already being tapped and this offers a large scope for the development of this low wind speed turbines. Our study focuses primarily on designing the blade for tapping power in the regions of low wind power density. The aerodynamic profiles of wind turbine blades have crucial influence on aerodynamic efficiency of wind turbine. This involves the selection of a suitable airfoil section for the proposed wind turbine blade. The NACA 63 series is chosen as the basic group for investigation because they have good low speed characteristics and the power curve is better in the low and medium wind speed ranges. In this paper NACA 63-415 airfoil profile is considered for analysis of wind turbine blade. NACA 63-415 airfoil profile is created by using the co-ordinate file generated in JavaFoil. A C-Mesh Domain for the fluid around the airfoil is created using Design Modeler in ANSYS Workbench. The CFD analysis is carried out using STAR-CCM+ at various angles of attack from 0^0 to 16^0. The coefficient of lift and drag values are calculated for low Reynolds number and the pressure distributions are also plotted. The airfoil NACA 63-415 is analyzed based on computational fluid dynamics to identify its suitability for its application on wind turbine blades and good agreement is made between results.

Keywords: Lift, Drag, NACA, CFD, Wind Turbine Blade And Renewable Energy.

NOMENCLATURE

C_L	Lift coefficient
C_D	Drag coefficient
α	Angle of attack
ρ	Air density
r	Local blade radius
C	Blade chord
θ	Twist angle
φ	Inflow angle
ω	Blade angular velocity
a	Axial induction factor
V_o	Wind velocity at hub height
V_{rel}	Resultant wind velocity

1 Introduction

Wind energy has been one of the most viable sources of renewable energy. The low cost of wind energy is competitive with more conventional sources of energy. As a sustainable energy resource, wind energy is increasingly important in national and international energy policy in response to climate change. A wind turbine is a machine which converts the power in the wind into electricity. The subsystems of a wind turbine include the rotor, the drive train, the nacelle and main frame, the machine controls, the electrical system, the tower and the foundation. The rotor consists of the blades and the supporting hub.

Wind turbine blade profiles are often constructed using a combination of 2-D airfoil tools and the Blade Element Momentum (BEM) theory. BEM theory gives the angle of twist and chord length for a given cross section of the airfoil and rotation speed at a finite number of positions along the blade span. A three dimensional shape can be extruded from these two dimensional sections. The BEM theory considers a given airfoil cross section as independent, then processes the wind with a speed and direction that is obtained from vector sum of the oncoming wind speed and the wind speed generated by rotor rotation. Unlike aerodynamic studies on higher Reynolds number flows, the numerical or analytical study of flows at very low Reynolds numbers is not quite matured. The 2D airfoil geometries are considered for study to understand the low Reynolds number flow [1].

1.1 Wind Power

The amount of energy in a column of wind seen by the swept area of a turbine can be found from its kinetic energy and the power is expressed as follows [2]

$$P_{avail} = \frac{1}{2}\dot{m}V_o^2 = \frac{1}{2}\,\rho A V_o^3 \tag{1}$$

where $\dot{m}$ is mass flow rate of air through a rotor disc and A is the area swept by the rotor

1.2 Wind Power Density

Power per unit area available from steady wind [3]

$$\frac{P_{avail}}{A} = \frac{1}{2}\,\rho V_o^3 \tag{2}$$

Table 1. Wind Power Density

Wind Speed (m/s)	Wind Power Density (W/m^2)
0	0
5	80
10	610

When wind power density is less than 100 W/m^2, the region falls under the zone of low wind speed region. The objective of this study is to design the blade for tapping wind power in such regions.

1.3 Lift and Drag

Lift force is the force perpendicular to direction of the oncoming air flow as a consequence of the unequal pressure on the upper and lower airfoil surfaces.

Drag force is the force parallel to the direction of the oncoming air flow due both to viscous friction forces at the surface of the airfoil and to unequal pressure on the airfoil surfaces facing toward and away from the oncoming flow.

Pitching moment acts about an axis perpendicular to the airfoil cross-section.

$$Lift = \frac{1}{2} * \rho * C_L * c * L * V_{rel}^2 \tag{3}$$

$$Drag = \frac{1}{2} * \rho * C_D * c * L * V_{rel}^2 \tag{4}$$

where ρ – Density of air - 1.225 kg/m^3
c – Chord length
L – Length of the blade element
V_{rel} – Relative velocity of air

$$V_{rel} = \sqrt{V_o^2 + (r\omega)^2} \tag{5}$$

1.4 NACA 6-series airfoil

The NACA 63 series is chosen as the basic group for investigation because they have good low speed characteristics with a minimum compromise from consideration of the high speed characteristics [4]. For NACA 63 series airfoil profiles, the power curve is better in the low and medium wind speed ranges, but drops under operation at higher wind speeds [5].

The NACA 6-series airfoil is described using six digits in the form NACA 65_3-421 where the number "6" indicates the series [6]. The second digit describes the distance of the minimum pressure area in tens of percent of chord. Here the area of minimum pressure is 50% of the chord back. The subscript 3 means that the drag coefficient is near its minimum value over a range of lift coefficients of 0.3 above and below the design lift coefficient, the next digit indicates the lift coefficient in tenths (here, 0.4) and the last two digits give the maximum thickness in percent chord (here, 21% of chord).
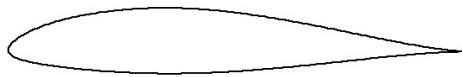
Fig. 1. NACA 63-415 Airfoil created from JavaFoil
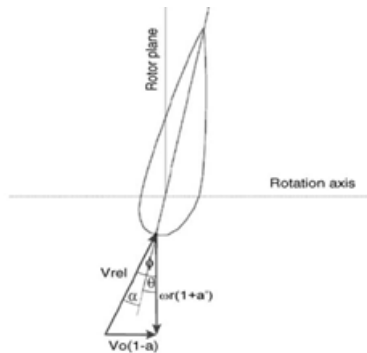
Fig. 2. Blade velocity diagram

For NACA 63 series airfoil profiles the parameters that are to be considered for selection are the design lift coefficient and the maximum thickness in percent chord.


3
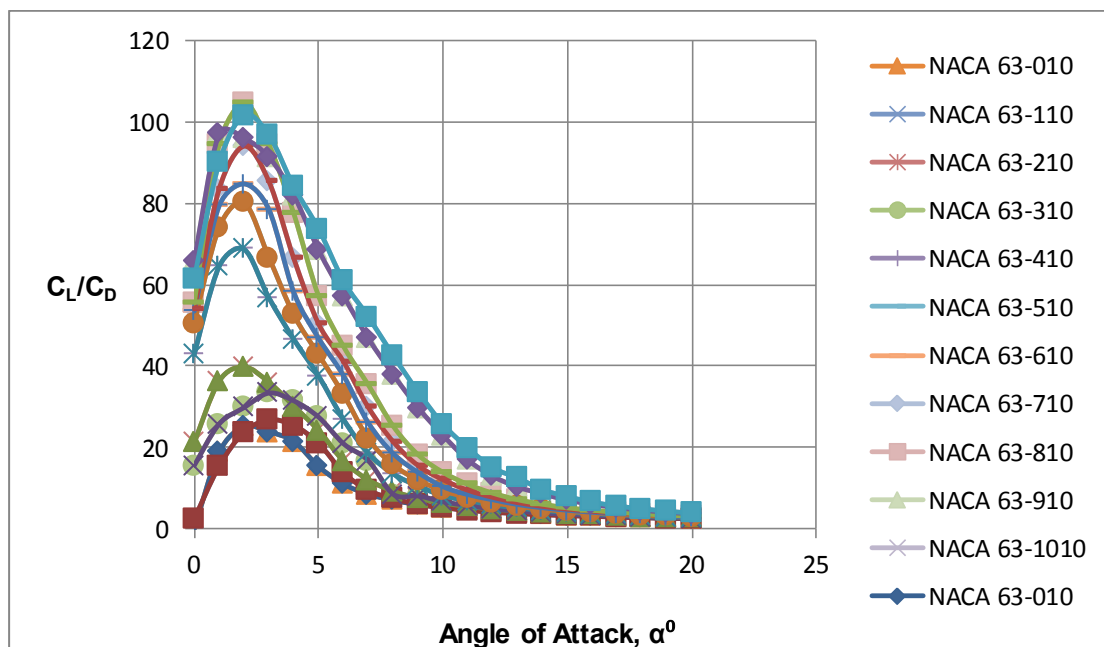
Fig. 3. C_L / C_D Vs Angle of attack for varying Design Lift Coefficient

The NACA 63 series profiles with design lift coefficient up to 0.3 have low C_L / C_D ratio. So profiles with design lift coefficient greater than 0.3 are considered for selection. Among these the profiles NACA 63-410 is found to have a low pitching moment coefficient.
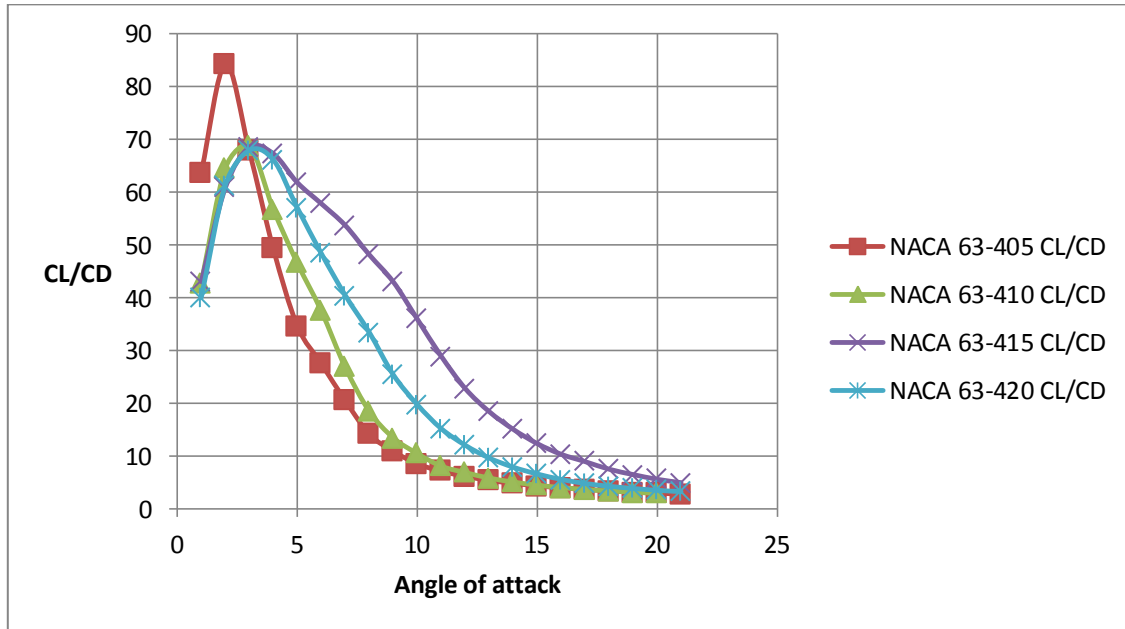

Fig. 4. C_L / C_D Vs Angle of attack for varying Thickness in percentage of chord

For the design lift coefficient of 0.4, NACA profiles of various thicknesses are analysed. The profile with maximum thickness of 15% of the chord has high C_L / C_D ratio for a wide range of angle of attack.

The design lift coefficient of 0.4 and maximum thickness of 15% of the chord have been selected for the analysis by taking into consideration the stalling characteristics which occur due to flow separation.

The values of C_L and C_D were found out for various angles of attack. The C_L/C_D ratio is calculated for different angle of attack ranges from 0^0 to 16^0. The values of the ratio of lift and drag coefficient for different NACA 63-415 airfoil profile is given in Table.2. The lift and drag coefficient for the different angle of attack is plotted in Fig.5 and 6. The correlation between coefficient of lift and coefficient of drag is shown in Fig.7.

Table 2. C_L / C_D ratio for NACA 63-415

Angle of Attack	C_L	C_D	C_L / C_D
0	0.2572784424	0.006420399062	40.07203
1	0.3818179667	0.006230164785	61.28537
2	0.5074353814	0.00747021148	67.92785
3	0.6297262311	0.009552824548	66.12809

Angle of Attack	C_L	C_D	C_L / C_D
4	0.7455788851	0.01306486502	57.06748
5	0.8505649567	0.01756297983	48.42942
6	0.934704423	0.02309199609	40.47742
7	1.006961703	0.03007490747	33.48179
8	1.030676842	0.04048165306	25.46034
9	1.016640425	0.05133248121	19.80501
10	1.005674601	0.0659379065	15.25184
11	0.9917430878	0.08196154237	12.1001
12	0.9724330306	0.1004771516	9.678151
13	0.9495124221	0.119452998	7.948837
14	0.9389573336	0.1411192864	6.653643
15	0.9262664318	0.1643468142	5.636047
16	0.919416368	0.1893396676	4.85591
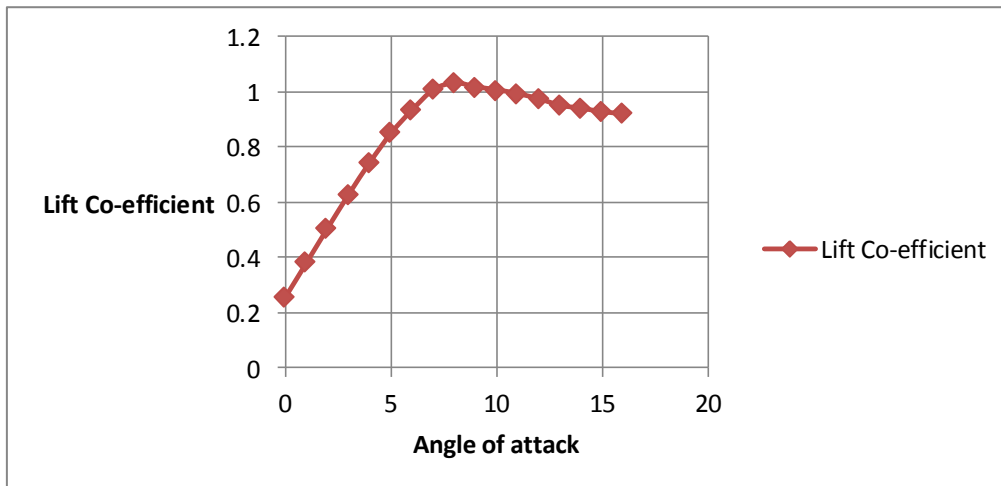
Fig. 5. Lift Coefficient Vs Angle of attack
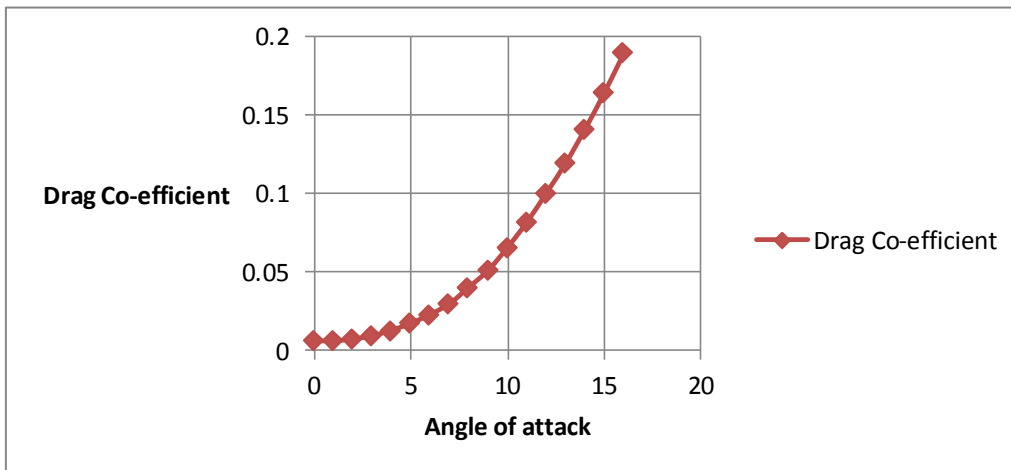
Fig. 6. Drag Coefficient Vs Angle of attack
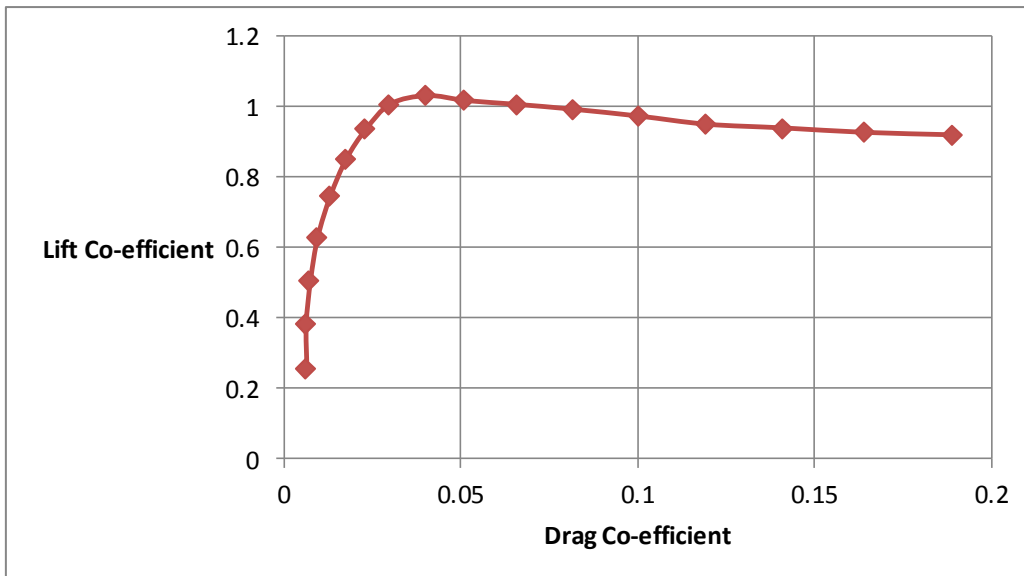
Fig. 7. Correlation between C_L and C_D

2 COMPUTATIONAL FLOW ANALYSIS

The airfoil NACA 63-415 is chosen for analysis as shown in fig.1. The airfoil profile and boundary conditions are all created. NACA 6-series profiles are obtained from Javafoil. A C-Mesh Domain for the fluid around the airfoil is created using Design Modeler in ANSYS Workbench. A smart fine mesh is created for the flow area.of the fluid domain in ANSYS Workbench.Computational fluid dynamic analysis of the flow around the airfoil is done using STAR CCM+.

The models created in STAR CCM+ define the spatial and temporal solution methods and the physical properties of the flow. In the analysis, the flow is steady, turbulent and compressible. The Spalart-Allmaras turbulence model and the ideal gas model are used for analysis.

Inlet velocity for the simulations is 30 m/sec which is the relative velocity calculated from $V_{rel} = V_o\sqrt{1 + \lambda^2}$ where the wind velocity and tip speed ratio are taken as 4 m/s and 7.5 respectively. A fully turbulent flow solution was used in STAR-CCM+, where Spalart-Allmaras equation was used for turbulent viscosity and the turbulence viscosity ratio is set to10.
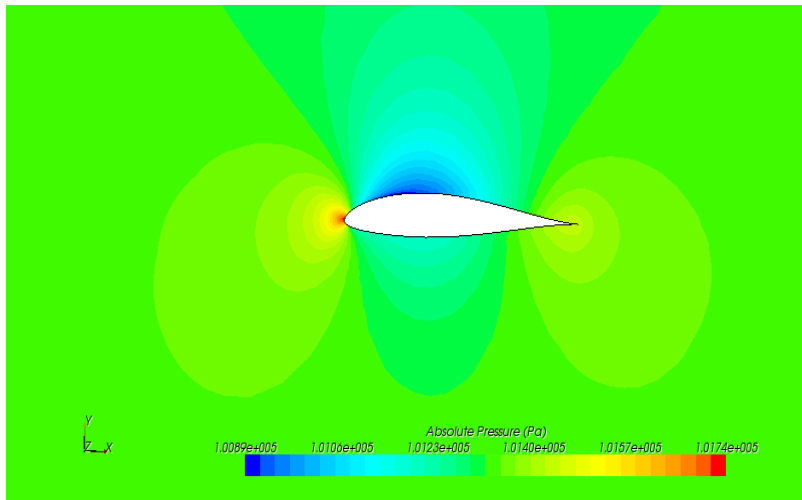
**Fig. 8**. Pressure plot – 0° Angle of attack
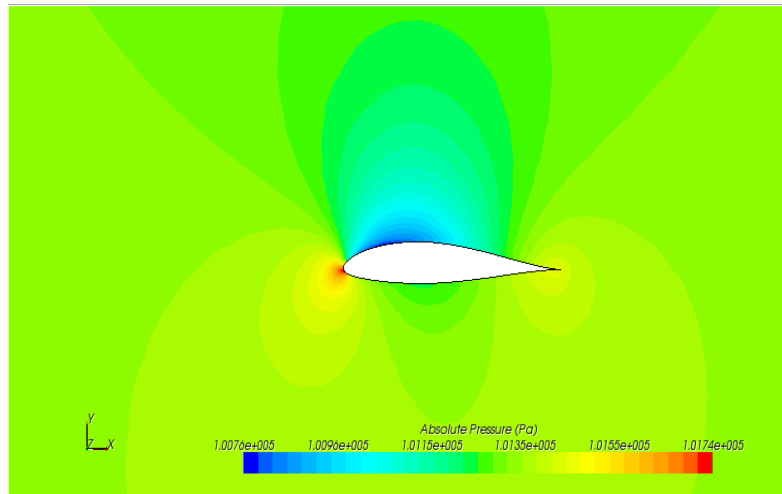

Fig. 9. Pressure plot – 2° Angle of attack
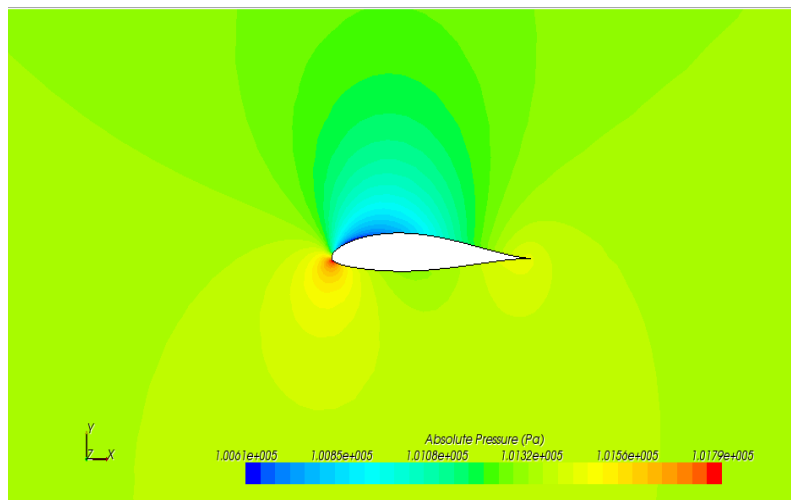
**Fig. 10.** Pressure plot – 4° Angle of attack
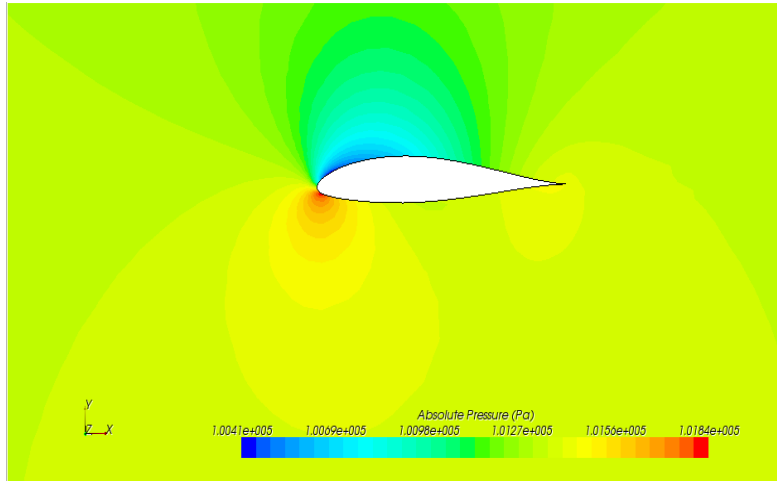
Fig. 11. Pressure plot – 6° Angle of attack
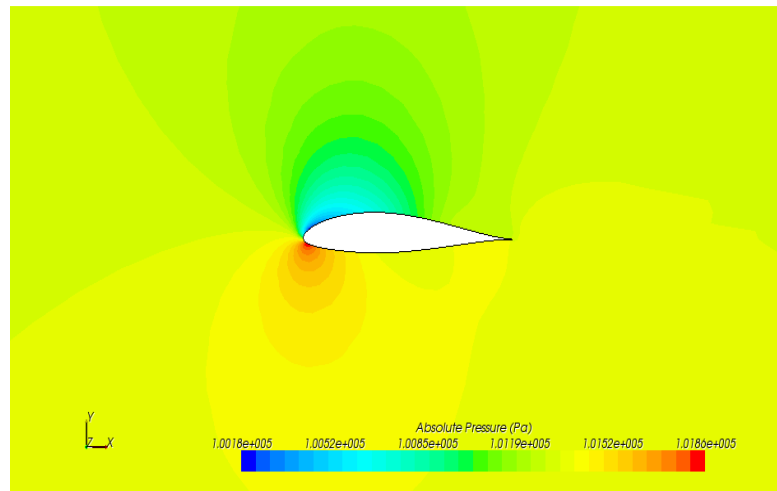

Fig. 12. Pressure plot – 8° Angle of attack
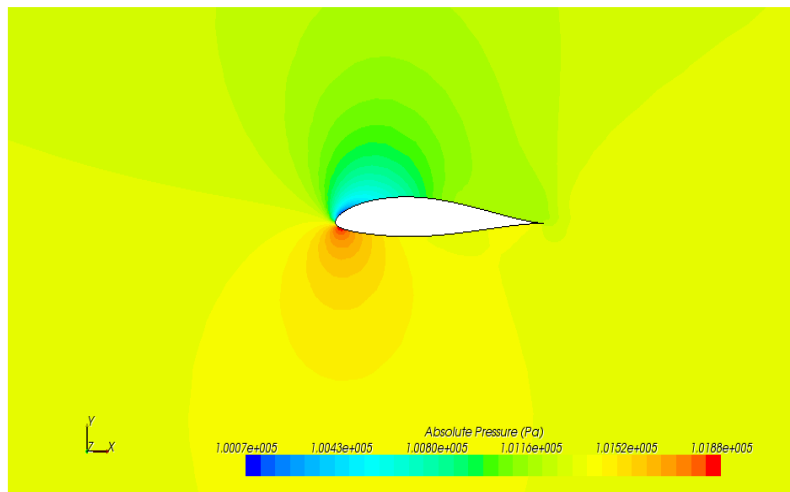
**Fig. 13.** Pressure plot – 10° Angle of attack
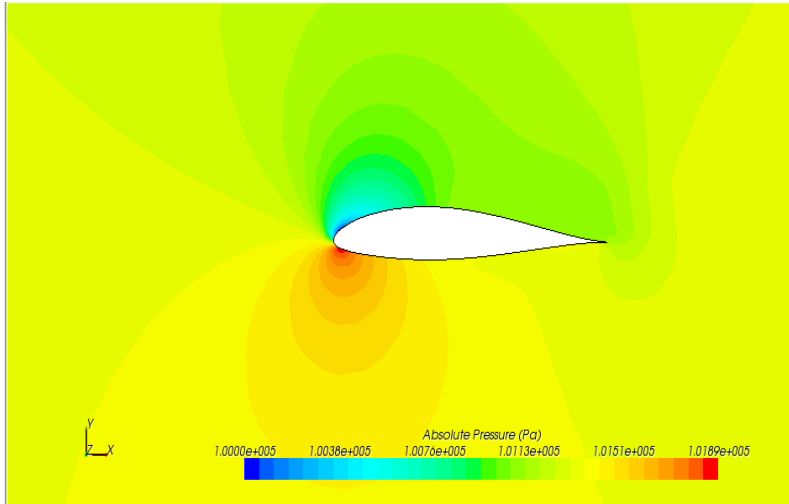
**Fig. 14.** Pressure plot – 12° Angle of attack
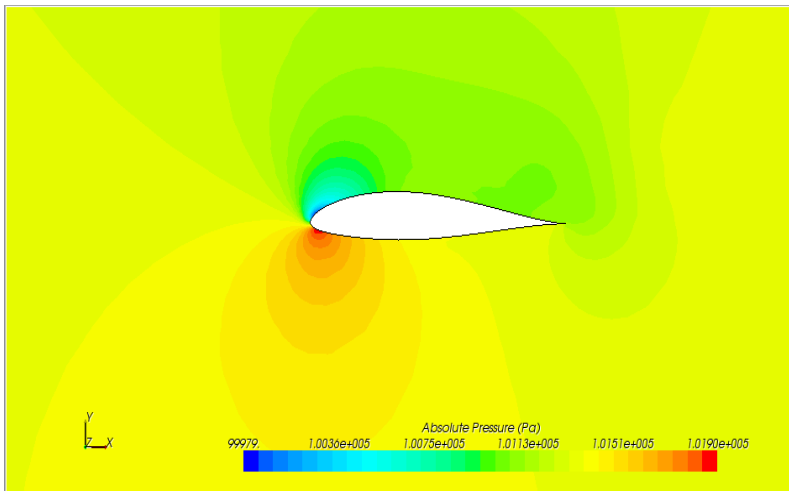
**Fig. 15.** Pressure plot – 14° Angle of attack
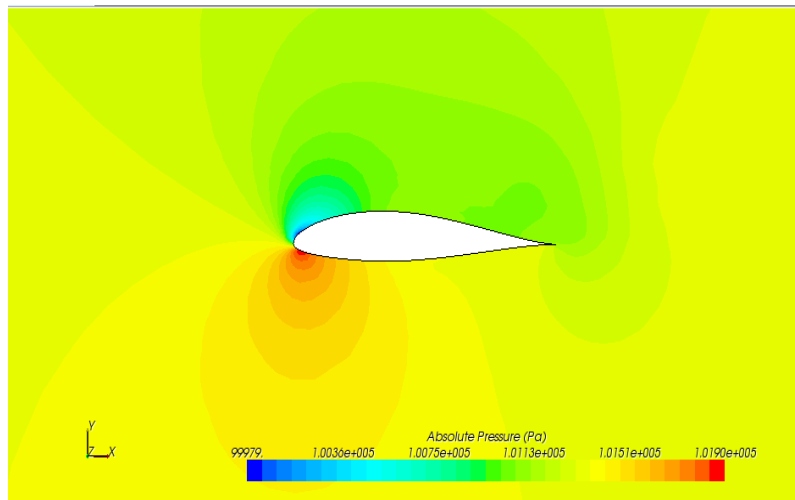
Fig. 16. Pressure plot – 16° Angle of attack

3 RESULTS

In this paper a Horizontal axis wind turbine blade profile NACA 63-415 is analyzed for various angles of attack. The coefficient of Lift and drag is calculated for this NACA 63-415 for various angles of attack from 0° to 16° and the maximum C_L/C_D ratio is achieved at 2° of angle of attack. The coefficient of Lift increases with increase in angle of attack up to 8°. After 8°, the coefficient of lift decreases and stall begins to occur. The drag forces begin of dominate beyond this angle of attack. The rate of increase in lift is more for angle of attack from 0° to 8° and then it starts to decrease. The drag increase gradually until 5° angle of attack and then rapidly increases. The CFD analysis is carried out using STAR-CCM+ software. The pressure distribution at various angles of attack of the blade is shown in Fig. 8-16. These results are compared with the wind tunnel experimental values for validation [7].

References

1. Kunz, Peter J., Kroo, Ilan M.: Analysis, design and testing of airfoils for use at ultra-low Reynolds numbers. Proceedings of the Conference on Fised, Flapping and Rotary Vehicles at very Low Reynolds Numbers, Univ. of Notre Dame, Notre Dame, IN, pp.349-372 (2000)
2. Hasen M.: Aerodynamics of Wind Turbines.
3. Manwell, J.F., McGowan, J.G., Rogers, A.L.: Wind Energy Explained, Theory, Design and Application, 2nd ed., John Wiley and Sons Ltd., New York (2009)
4. Loftin, Laurence K., Bursnall, William J.: The Effects of Variation in Reynolds Number between 3.0 X 10^6 and 25.0 X 10^6 upon the Aerodynamic characteristics of a number of NACA 6-Series Airfoil Sections.
5. Henrik Stiesdal: Bonus-Info - The Wind Turbine Components and Operation.
6. Kuethe, Schetzer: Foundations of Aerodynamics, 2nd ed., John Wiley and Sons Ltd., New York (1959)
7. Christian Bak, Peter Fuglsang, Jeppe Johansen, Ioannis Antoniou: Wind Tunnel Tests of the NACA 63-415 and a Modified NACA 63-415 Airfoil. Riso National Laboratory, Denmark.